A Simple Method to Estimate Coil Temperature with Local Normal-State Region

Takanobu Mato and So Noguchi, *Member, IEEE*

***Abstract*— This paper proposes a simple analytical expression to estimate the temperature of no-insulation (NI) high-temperature superconducting (HTS) coils when a local normal zone appears. The combination of the NI winding technology and HTS, especially rare-earth barium copper oxide (REBCO), enables high-field generation with high thermal stability. Since the advent of the NI winding technology, a few simulation techniques have been improved: the finite element method (FEM) and the partial element equivalent circuit (PEEC) are well-established as of today. The PEEC method can simulate the coil behaviors relatively fast compared with the FEM simulation due to the number of elements. However, the computation time is still long, particularly when a normal-state transition is simulated coupled with thermal analysis due to the extreme non-linearity of the superconductors. Therefore, we have previously proposed a simple and versatile analytical expression to estimate NI HTS coil temperatures in the cases of ramping down with an arbitrary speed and sudden discharging. Compared with PEEC simulations, the analytical formulae were validated in both cases under the assumption that the NI HTS coil is perfectly superconducting. In this paper, taking further realistic considerations into account, an NI HTS coil with a few normal-state turns is modeled, and its temperature is also formulated. The calculation results are validated with the PEEC model, and the accuracy and usable range of the proposed method is also discussed.**

***Index Terms*—HTS magnet, no-insulation winding technique, simple evaluation, thermal stability.**

I. Introduction

NO-INSULATION (NI) high-temperature superconducting (HTS) coils have been paving the way toward high-field applications. As a matter of fact, an NI rare-earth barium copper oxide (REBCO) coil as an insert coil has generated 14.4 T under a background field of 31.1 T with a resistive magnet [1]. Following the experiment of 45.5 T generation, several institutes employed NI-related technologies towards the generation of high fields [2]-[5]. The NI REBCO coils exhibit potential for high-field applications, whereas the NI REBCO coils demonstrate complexities in their current distribution due to the capability of current sharing among the turns [6]. The complicated current behaviors are one of the major obstacles to coil designs and further developments.

As of today, several simulation techniques have been developed to evaluate the behaviors of NI REBCO coils. For example, finite element methods (FEM) are a powerful tool to precisely simulate screening current distribution and the consequent deformation [7]-[9]. The partial equivalent element circuit (PEEC) method is also widely used such as in the simulation of the normal-state transition and the current distribution of various operations [10]-[13]. The PEEC method has a feature of faster computation than the FEM; nevertheless, significant coding is required. Thus, we previously proposed a simple analytical expression to estimate the temperature of the NI HTS coils during ramp-down and sudden-discharge operations [14]. An NI HTS coil was modeled with a simple RL circuit, then the coil currents were formulated, followed by the coil temperature formulation considering the cooling effect. It was demonstrated that the simple analytical expression could well estimate the temperature of the NI REBCO coil with almost zero computation time. The estimation results were validated by comparing them with the PEEC simulation results. However, the analytical expression was obtained under the assumption of a perfectly superconducting state.

In this paper, the currents and temperatures of an NI HTS coil having local normal-state zones are analytically formulated to impose further realistic features on the modeling, where its simplicity and conciseness are retained well. The formulation is aimed at the rough calculation of robustness against hot-spot appearance, not at the detailed simulation. The calculation results are validated with the well-established PEEC model, and the accuracy and usable range of the proposed method are also discussed.

II. Formulation of Current and Temperature

A. Coil Current

Now, we consider the case where a local normal-state zone appears in an NI HTS coil and the operation current decreases to zero. The coil current during ramp down is formulated, followed by the coil temperature formulation. Now, we assume an NI HTS coil as shown in Fig. 1(a). The NI HTS coil has a small normal-state region at the middle turns of the coil, surrounded by the superconducting turns. The equivalent circuit of the NI HTS coil is represented in Fig. 1(b). The superconducting turns at the inner and outer parts have the inductances L_1 and L_2, and the turn-to-turn contact resistance

Manuscript received. This work was supported by the JSPS KAKENHI under Grant No. 22KJ0104. (Corresponding author: Takanobu Mato.)

T. Mato and S. Noguchi are with the Faculty of Information Science and Technology, Hokkaido University, Sapporo, 060-0814 Japan (e-mail: e-mail: mato@ist.hokudai.ac.jp, noguchi@ssi.ist.hokudai.ac.jp).

Color versions of one or more of the figures in this article are available online at http://ieeexplore.ieee.org

Digital Object Identifier will be inserted here upon acceptance.

R_{r1} and R_{r2}. The normal-state region has the inductance L_n, the circumferential resistance R_{Ln}, and the turn-to-turn contact resistance R_{rn}. The calculation of contact resistance is expressed as follows

$$R_{rx} = \sum_{i=1}^{N_x} \frac{\rho}{S_i},$$

where, N is the number of turns at superconducting or normal regions, ρ is the contact resistivity, and x represents 1, 2, or n.

Now, the inductance at the normal-state region is neglected since the inductance is very low compared with the other inductances L_1 and L_2, a few hundred μH in the model case in this paper. Thereby, the circuit is simplified as shown in Fig. 1(c). The inductance L is a coil inductance, and the coil contact resistance R_r and the normal-state region resistance R_n are calculated as follows:

$$R_r = R_{r1} + R_{r2}, \tag{1}$$

$$R_n = \frac{R_{Ln} R_{rn}}{R_{Ln} + R_{rn}}. \tag{2}$$

Fig. 2 shows the power supply profile. Initially, the power supplies I_m to the coil, then after $t = 0$, the power supply begins to decrease its output with the ratio r [A/s]. Thus, operating current I_{op} is defined as the following equation:

$$I_{op} = \begin{cases} I_m - rt & (0 \le t < t_0) \\ 0 & (t_0 \le t) \end{cases}, \tag{3}$$

where t_0 is the time when the operating current reaches zero. Here, setting a very high sweep rate corresponds to open-circuit dumping [14].

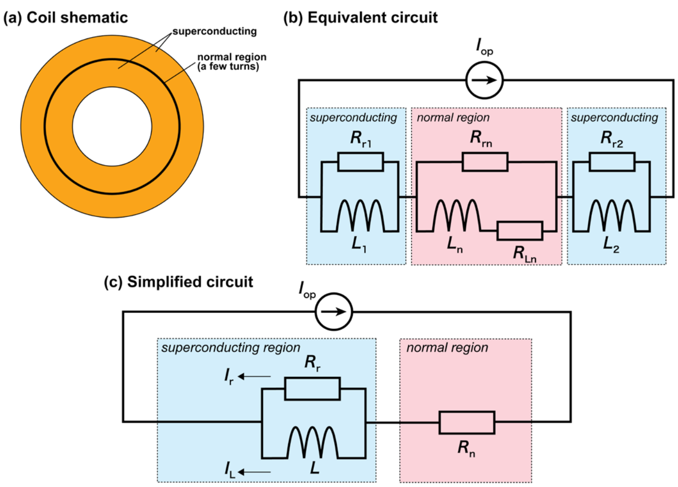

Fig. 1. (a) NI HTS coil with normal-state turns, (b) electrically equivalent circuit, and (c) simplified circuit.

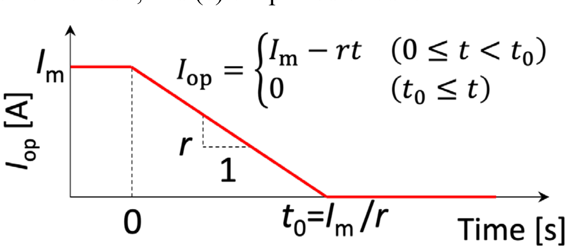

Fig. 2. Power supply current for ramp down operation.

Now we derive the coil current during the ramp down operation. The governing equation is given by

$$L \frac{dI_L}{dt} + R_r (I_L - I_{op}) = 0. \tag{4}$$

By solving the governing equation under the initial condition $I_L = I_m$ at $t = 0$, we get the circumferential current and the radial current:

$$I_L = \begin{cases} r\tau_e \left(1 - e^{-\frac{t}{\tau_e}}\right) + I_{op} & (0 \le t < t_0) \\ r\tau_e \left(e^{-\frac{t-t_0}{\tau_e}} - e^{-\frac{t}{\tau_e}}\right) & (t_0 \le t) \end{cases}, \tag{5}$$

$$I_r = \begin{cases} -r\tau_e \left(1 - e^{-\frac{t}{\tau_e}}\right) & (0 \le t < t_0) \\ -r\tau_e \left(e^{-\frac{t-t_0}{\tau_e}} - e^{-\frac{t}{\tau_e}}\right) & (t_0 \le t) \end{cases}. \tag{6}$$

Note that the τ_e is the time constant of the NI HTS coil, which is calculated as $\tau_e = L/R_r$.

B. Coil Temperature

In the coil temperature formulation, the following are assumed: (i) the coil is immersed in the coolant of temperature T_c, (ii) the coil is cooled according to Fourier's law with a constant heat transfer coefficient h [W/(K·m^2)], and (iii) the superconducting and the normal-state regions are thermally decoupled. The temperatures of the superconducting region T_s and the normal-state region T_n are then governed by the following equations:

$$C_s \frac{dT_s}{dt} = R_r I_r^2 - H_s (T_s - T_c), \tag{7}$$

$$C_n \frac{dT_n}{dt} = R_n I_{op}^2 - H_n (T_n - T_c), \tag{8}$$

where C is the heat capacity, and the subscripts s and n denote the superconducting and the normal-state regions, respectively. Also, H [W/K] is the heat transfer coefficient given by hS , where S is the interface area between the coolant and the coil. The thermal properties are found in [15].

First, the governing equation of the superconducting region (7) is solved under $T_s(0) = T_c$ and we obtain

$$T_s(t) = \begin{cases} f_s(t) - f_s(0) e^{-\frac{t}{\tau_{hs}}} + T_c & (0 \le t < t_0) \\ g_s(t) + \left(f_s(t_0) - g_s(t_0)\right) e^{-\frac{t-t_0}{\tau_{hs}}} \\ \quad -f_s(0) e^{-\frac{t}{\tau_{hs}}} + T_c & (t_0 \le t) \end{cases}. \tag{9}$$

Note that τ_{hs} is the time constant related to cooling, defined as C_s/H_s. The functions $f_s(t)$ and $g_s(t)$ are given below:

$$f_s(t) = \frac{R_r}{H_s} r^2 \tau_e^2 \left(1 - \frac{2\tau_e}{\tau_e - \tau_{hs}} e^{-\frac{t}{\tau_e}} + \frac{\tau_e}{\tau_e - 2\tau_{hs}} e^{-\frac{2t}{\tau_e}}\right), \tag{10}$$

$$g_s(t) = \frac{R_r}{H_s} \frac{\tau_e}{\tau_e - 2\tau_{hs}} I_r^2. \tag{11}$$

Similarly, the temperature of the normal-state region is obtained as follows:

$$T_{\mathrm{n}}(t)=\begin{cases} f_{\mathrm{n}}(t)-f_{\mathrm{n}}(0)e^{-\frac{t}{\tau_{\mathrm{hn}}}}+T_{\mathrm{c}} & (0\le t<t_0) \\ f_{\mathrm{n}}(t_0)e^{-\frac{t-t_0}{\tau_{\mathrm{hn}}}}-f_{\mathrm{n}}(0)e^{-\frac{t}{\tau_{\mathrm{hn}}}}+T_{\mathrm{c}} & (t_0\le t) \end{cases}, \quad (12)$$

where the time constant τ_{hn} is defined as $C_{\mathrm{n}}/H_{\mathrm{n}}$. The function $f_{\mathrm{n}}(t)$ are

$$f_{\mathrm{n}}(t)=\frac{R_{\mathrm{rn}}}{H_{\mathrm{n}}}\left(\left(I_{\mathrm{op}}+r\tau_{\mathrm{hn}}\right)^2+r^2\tau_{\mathrm{hn}}^2\right). \quad (13)$$

It is worth mentioning modeling of the innermost or outer turn quench is possible by changing the radial resistance at normal turn R_{n}. Changing the number of normal turns, which indicates the delay of quench detection, also affects the estimated temperature.

III. Result Comparison with PEEC Simulation

A. Coil Voltage

In order to check the validity of the derived formulae, we compare the results obtained from the proposed formulae and the PEEC simulations [16]. The specifications of the NI REBCO coil which are supposed to be simulated are shown in Table I. The coil parameters and the operating conditions are referred from the previous work [14]. In the formula calculation and the PEEC simulation, the central 5 turns inside the NI REBCO coil (98th to 102nd turns from inner) transition to the normal state at t = 0, and then, the operating current is decreased at 100 A/s as shown in Fig. 2.

TABLE I
Coil Specifications and Operation Parameters

Parameters	Values
I.D.; O.D.; Height [mm]	50; 90; 4.0
Number of turns	200
Number of single pancakes	1
Initial operating current [A]	268.6
Magnetic field [T]	7 (background 5 T)
Coil inductance [mH]	3.48
Coil heat capacity [J/K]	15.8
Coolant temperature [K]	4.2
Heat transfer coefficient [W/(K·m^2)]	100
Ramp down rate [A/s]	100
Number of normal-transitioned turns	5
Electrical time constant τ_{e} [s]	20.2@70 μΩcm·2
Thermal time constant τ_{hs}, τ_{hn} [s]	18.0, 15.0

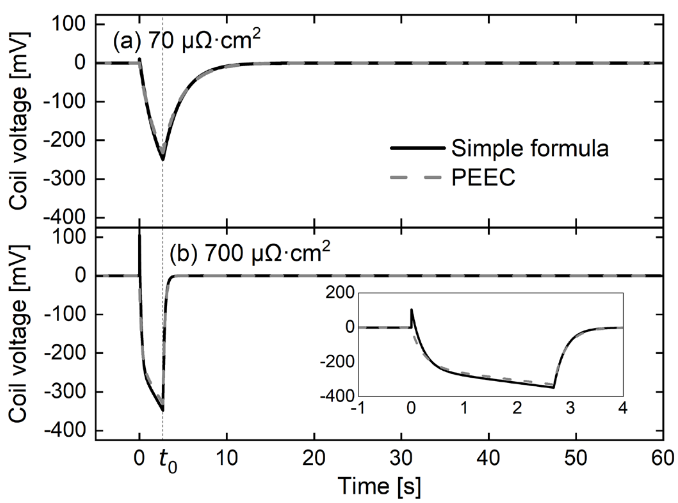

Fig. 3. Voltage behaviors of NI REBCO coil whose contact resistivity is (a) 70 μΩ·cm^2 and (b) 700 μΩ·cm^2. The solid and the broken lines correspond to the simple formula calculation and the PEEC simulation, respectively.

We first calculate the coil voltage using the following equation:

$$V_{\mathrm{coil}}=R_{\mathrm{r}}I_{\mathrm{r}}+R_{\mathrm{n}}I_{\mathrm{op}}. \quad (14)$$

Fig. 3 shows the voltage of the NI REBCO pancake coil with contact resistivities of 70 and 700 μΩ·cm^2 after the normal-state turn appearance. It is important to note that the calculation of the proposed method for the voltage and the subsequent temperature was completed in a remarkably short time, only a few milliseconds. The coil voltages well agree in both cases. It means that the coil current of the NI REBCO pancake is well modeled even when a hot spot appears. It is noted that a voltage spike appears at t = 0 in the case of 700 μΩ·cm^2 of the proposed formula as can be seen in Fig. 3(b). This is because the inductance of the normal-transitioned area is ignored, that is, the negative voltage to cancel the rapid voltage increase at the normal-transitioned area is not induced in the superconducting region.

B. Coil Temperature

The coil temperature is estimated with (9) for the superconducting region and (12) for the normal-transitioned region. Fig. 4 illustrates the averaged coil temperature (black) along with the temperature at the normal-transitioned region (red). When the contact resistivity is 70 μΩ·cm^2, the averaged coil temperatures behave in the same way in both methods. Particularly, it is important that both methods estimate the maximum temperature of the normal-transitioned area to be approximately 10 K. This result demonstrates the proposed model is correctly modeled in this condition.

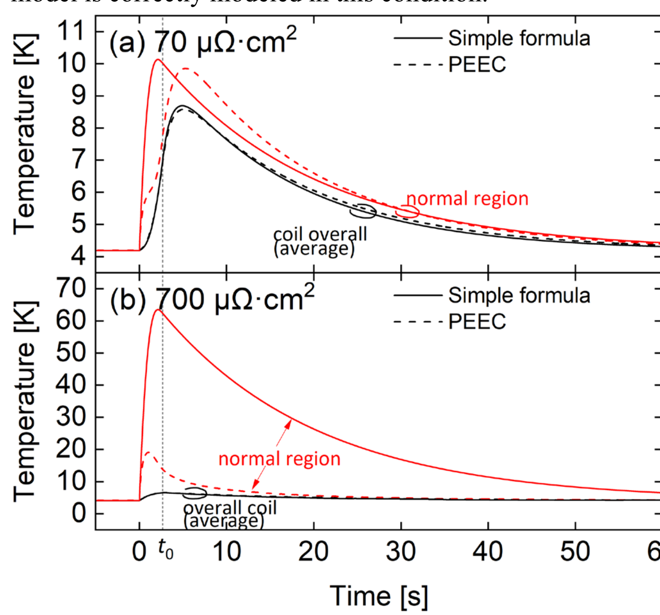

Fig. 4. Temperature of normal-transitioned region (red) and overall coil (black) in the case where the contact resistivity is 70 and 700 μΩ·cm^2.

In the case of 700 μΩ·cm^2, a large discrepancy is observed in the normal-transitioned region. The PEEC simulation estimates the maximum temperature to be 19 K, while the proposed formula estimates it as 64 K. To reveal the detailed mechanism of the different estimated temperatures, the temperature distribution inside the NI REBCO pancake coil computed with the PEEC method is plotted in Fig. 5. At 1 s after the normal-state zone appearance, the temperature at the middle turns of the coil reaches 19 K. It is evident that the temperature increases not only at the normal-transitioned turns but also at the adjacent superconducting turns; e.g., the closest turns to the normal-transitioned region reaches 15.1 K. This is because some of the generated heat is diffused to adjacent regions. After t = 1 s, the temperature of the normal-transitioned turns decreases due to the thermal diffusion and the cooling effect. However, the proposed model does not consider the thermal conduction inside the NI REBCO pancake coil, which leads to the discrepancy and overestimation of the maximum temperature.

Further verification is performed to see the limitations of the proposed equations. Fig. 6(a) shows the averaged coil temperature (black) and the temperature range (blue shaded area) as a function of the contact resistivity, computed with the PEEC simulation. Here, the temperature range is defined as a difference between the maximum and the minimum of the reached temperature during operations. Meanwhile, Fig. 6(b) shows the maximum temperature at the normal-transitioned area (red) and on the whole coil (black) estimated with the proposed simple formulae. At a high ramp down speed, e.g. 1000 A/s, the averaged coil temperatures of Fig. 6(a) and (b) are almost identical. As for the temperature of the normal-state region, it tends to be underestimated with the simple formula. At the other ramp rates, 1, 10, and 100 A/s, the simple formula also well reflects the temperature increase of the PEEC simulated results: the temperature of the normal-state region in Fig. 6(b) changes similarly to the upper limit of the temperature range in Fig. 6(a). Therefore, the model is proven to be a useful tool to roughly estimate the thermal stability of the NI REBCO pancake coil when a hot spot appears, taking almost zero computation time and no effort to implement.

It is noted that the temperature estimation with the simple formula is not as accurate as the PEEC simulation when the amount of the Joule heat is large at the normal-state region. This is due to the decoupled thermal connection between the normal state and the superconducting region, as discussed earlier. This needs to be resolved as a future task.

IV. Conclusion

In this paper, we proposed a simple analytical expression to estimate the maximum temperature increase of NI REBCO pancake coils in the case of normal-state appearance with nearly zero computation time. The NI REBCO pancake coil having a few normal-state-transitioned turns is modeled as shown in Fig. 1(c), divided into the superconducting region and the normal-transitioned turns. The temperature estimation during ramp down operation after the appetence of normal-state-transitioned turns is performed with both the proposed formula and the PEEC simulation.

The results show that the proposed formula well estimates and reflects the electromagnetic behaviors. The temperature increase is also well modeled, whereas there is room for improvement in the qualitative accuracy, which could be achieved by considering the thermal conduction inside the NI REBCO pancake coil.

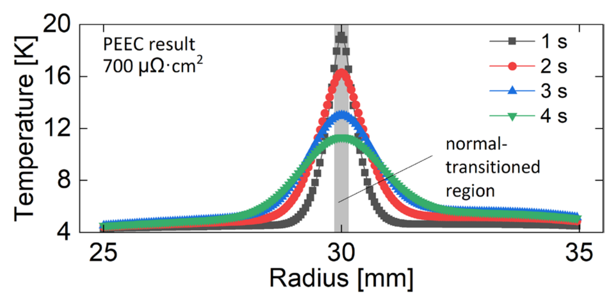

Fig. 5. Temperature distribution obtained from PEEC simulation in the case of 700 μΩ·cm^2.

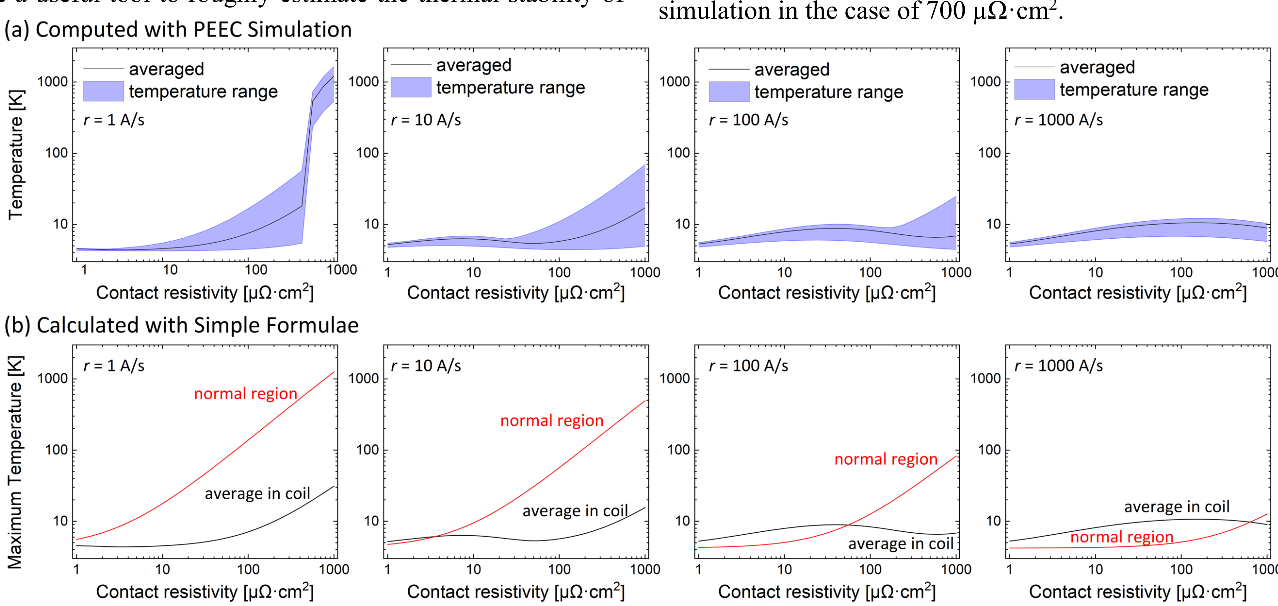

Fig. 6. Comparison of temperatures during ramp down operation at different sweep rate: (a) PEEC simulation results showing temperature range during current sweep and average temperature of coil and (b) results with proposed simple formulae.

REFERENCES

[1] S. Hahn et al., "45.5-Tesla Direct-Current Magnetic Field Generated with A High-Temperature Superconducting Magnet," *Nature*, vol. 570, no. 7762, pp. 496–499, 2019.

[2] Y. Suetomi et al., "Quench and Self-Protecting Behaviour of an Intra-Layer No-Insulation (LNI) REBCO Coil at 31.4 T," *Supercond. Sci. Technol*., vol. 34, no. 6, 2021, Art. no. 064003.

[3] D. Park et al., "MIT 1.3-GHz LTS/HTS NMR Magnet: Post Quench Analysis and New 800-MHz Insert Design," *IEEE Trans. Appl. Supercond.*, vol. 29, no. 5, 2019, Art. no. 4300804.

[4] S. Hahn et al., "A 78-mm/7-T Multi-Width No-Insulation ReBCO Magnet: Key Concept and Magnet Design," *IEEE Trans. Appl. Supercond*., vol. 24, no. 3, 2014, Art. no. 4602705.

[5] J. Liu et al., "World Record 32.35 Tesla Direct-Current Magnetic Field Generated with an All-Superconducting Magnet," *Supercond. Sci. Technol.*, vol. 33, no. 3, 2020, Art. no. 03LT01.

[6] A. Ikeda et al., "Transient Behaviors of No-Insulation REBCO Pancake Coil During Local Normal-State Transition," *IEEE Trans. Appl. Supercond*., vol. 26, no. 4, 2016, Art. no. 4600204.

[7] J. Bang et al., "The Effect of Field-Dependent n-Value on Screening Current, Voltage, and Magnetic Field of REBCO Coil," *IEEE Trans. Appl. Supercond*., vol. 34, no. 5, 2024, Art. no. 4902105.

[8] D. Kolb-Bond et al., "Screening Current Rotation Effects: SCIF and Strain in REBCO Magnets," *Supercond. Sci. Technol*., vol. 34, no. 9, 2021, Art. no. 095004.

[9] E. Pardo and P. Fazilleau, "Fast and Accurate Electromagnetic Modeling of Non-Insulated and Metal-Insulated REBCO Magnets," *Supercond. Sci. Technol.*, vol. 37, no. 3, 2024, Art. no. 035016.

[10] S. Noguchi and S. Hahn, "A Newly Developed Screening Current Simulation Method for REBCO Pancake Coils Based on Extension of PEEC Model," *Supercond. Sci. Technol*., vol. 35, no. 4, 2022, Art. no. 044005.

[11] T. Mato and S. Noguchi, "Axial Movement Effect on Voltage and Current Behaviors of Insert No-Insulation REBCO Pancake Coil," *IEEE Trans. Appl. Supercond*., vol. 33, no. 5, 2023, Art. no. 4602805.

[12] A. Gavrilin, D. Kolb-Bond, KL. Kim, K. Kim, W. Marshall, and I. Dixon, "Quench and Stability Modelling of a Metal-Insulation Multi-Double-Pancake High-Temperature-Superconducting Coil," *IEEE Trans. Appl. Supercond.*, vol. 31, no. 5, 2021.

[13] S. Noguchi, "Electromagnetic, Thermal, and Mechanical Quench Simulation of NI REBCO Pancake Coils for High Magnetic Field Generation," *IEEE Trans. Appl. Supercond*., vol. 29, no. 5, 2019, Art. no. 4602607.

[14] T. Mato and S. Noguchi, "A Simple and Versatile Evaluation Method of Thermal Stability of NI HTS Magnets," *IEEE Trans. Appl. Supercond*., vol. 34, no. 5, 2024, Art. no. 4700805.

[15] Y. Iwasa, Case Studies in Superconducting Magnets: Design and Operational Issues, 2nd ed. NY, USA: Springer Science+Business Media, 2009, pp. 359, 631-647.

[16] T. Mato and S. Noguchi, "Sudden Discharging and Overcurrent Simulations of REBCO Coils Coated with Conductive Epoxy Resin," *IEEE Trans. Appl. Supercond*., vol. 31, no. 5, 2021, Art. no. 4600705.